Journal of Magnetic Resonance 268 (2016) 88–94

Contents lists available at ScienceDirect

Journal of Magnetic Resonance

journal homepage: www.elsevier.com/locate/jmr

Determination of unresolved heteronuclear scalar coupling constants by *J*(up)-HSQMBC

Simon Glanzer [a], Olaf Kunert [b], Klaus Zangger [a,*]

[a] Institute of Chemistry/Organic and Bioorganic Chemistry, University of Graz, Austria
[b] Institute of Pharmaceutical Sciences/Pharmaceutical Chemistry, University of Graz, Austria

ARTICLE INFO

Article history:
Received 20 November 2015
Revised 25 February 2016
Accepted 5 May 2016
Available online 6 May 2016

Keywords:
NMR spectroscopy
J-upscaling
Band-selective decoupling
Homonuclear decoupling
HMBC
Structure analysis

ABSTRACT

Long-range heteronuclear scalar coupling constants provide important structural information, which is necessary for obtaining stereospecific assignment or dihedral angle information. The measurement of small proton–carbon splittings is particularly difficult due to the low natural abundance of carbon-13 and the presence of homonuclear couplings of similar size. Here we present a real-time *J*-upscaled HSQMBC, which allows the measurement of heteronuclear coupling constants even if they are hidden in the signal linewidth of a regular spectrum.

1. Introduction

NMR spectroscopy is one of the most powerful and frequently used tools for the analysis of small to medium sized molecules. Chemical shift, as well as scalar coupling information, play an important role for structural and conformational investigations. Long-range *J*-couplings are used to establish through-bond connectivities. They are necessary for example for the stereospecific assignment of carbon resonances attached to olefinic double bonds. Additionally, three-bond coupling constants provide information about dihedral angles through the Karplus relation [1]. However, the extraction of accurate and/or small coupling constants is often complicated, especially when they are smaller than the digital or spectral resolution. For proton–carbon coupling constants, the situation is made even more difficult by the low natural abundance of ^{13}C. While large one bond proton–carbon coupling constants ($^{1}J_{HC}$) can be determined easily from ^{13}C satellites, heteronuclear correlations exceeding one bond, with *J* values of ~0–15 Hz [2] are typically much more difficult to be measured [3–7]. The situation is further complicated by the similar magnitude of proton–proton and proton–carbon coupling constants. Such $^{n}J_{HC}$ ($n > 1$) can be measured for example by E.COSY type experiments [8,9], like the HETLOC (heteronuclear long-range couplings) [10–12]. Although the HETLOC and its modifications provide a relatively sensitive technique for the measurement of small heteronuclear couplings in TOCSY-like spectra, there are several shortcomings connected with it. Firstly, correlations are limited to ^{1}H–^{1}H spin systems and the intensity of the cross peaks are dependent on magnetization transfers over this homonuclear correlations. But the more severe problem is spectral overlap in both dimensions, which is due to the limited spectral range of hydrogen. For these reasons, experiments used for the detection and measurement of long-range proton–carbon couplings are mainly based on the HMBC experiment [13]. The determination of heteronuclear long-range couplings by direct inspection of HMBC peaks is basically impossible due to the evolution of homonuclear couplings during the pulse-sequence, combined with the anti-phase appearance of H–C couplings. Due to these complications, heteronuclear long-range coupling constants can only be obtained from HMBC spectra by line-shape fitting [14–17], which is made easier by avoiding proton–proton scalar coupling evolution [18–26] or by using the IPAP approach [27]. Heteronuclear long-range coupling constants can also be obtained from the indirect dimension of *J*-resolved HMBC spectra [28–30] or by recording series of HMBCs with different coupling evolution delays and analysis of signal intensities as a function of this delay – the quantitative HMBC [31,32]. One major problem of HMBC spectra is the limited resolution in the proton dimension. Pure shift NMR

* Corresponding author at: Institute of Chemistry/Organic and Bioorganic Chemistry, University of Graz, Heinrichstrasse 28, A-8010 Graz, Austria.
E-mail address: klaus.zangger@uni-graz.at (K. Zangger).

http://dx.doi.org/10.1016/j.jmr.2016.05.002
1090-7807/

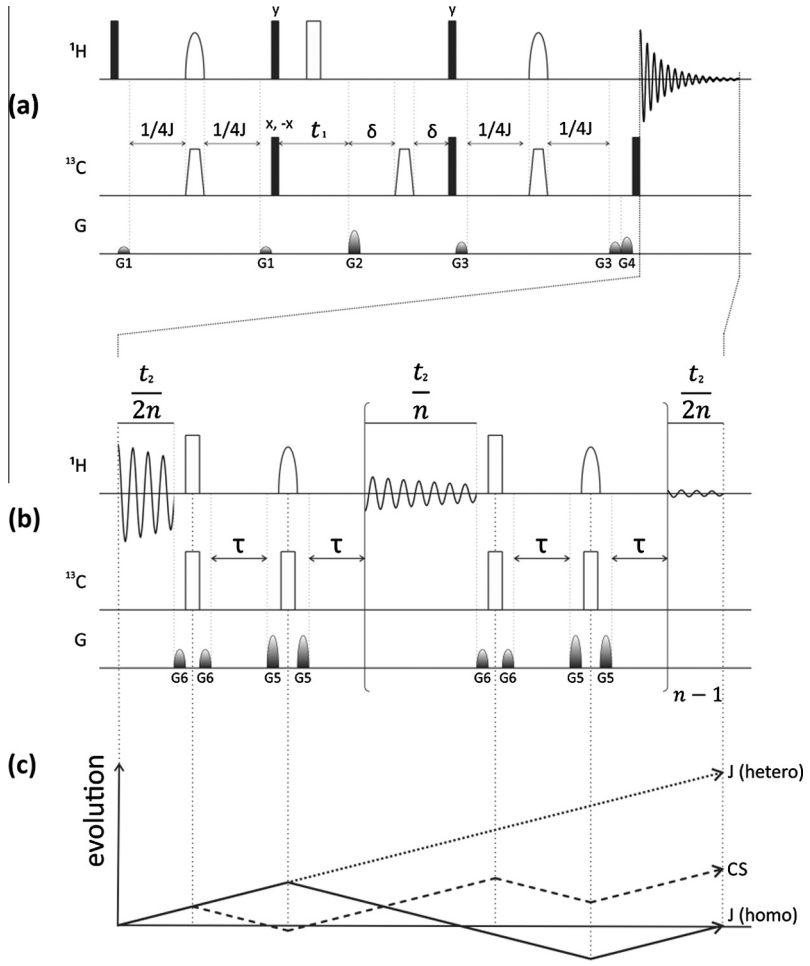

Fig. 1. (a) Pulse-sequence of the band-selectively decoupled *J*(up)-HSQMBC experiment. (b) A close-up view of the interrupted acquisition. Black and white bars are 90° and 180° pulses, respectively. Round shaped pulses are band-selective and trapezoidal-shapes are adiabatic pulses used for a uniform inversion over the full carbon spectral range. The following gradient ratios were used: G1:G2:G3:G4:G5:G6 = 11:80:17:20.1:63:41. All phases are *x*, unless indicated otherwise. (c) The evolution behavior of the different types of chemical shift (bold) as well as heteronuclear (dotted) and homonuclear (dashed) scalar coupling.

techniques by homonuclear broadband decoupling, have been described as a way to enhance the resolution of proton spectra [33–37]. Pure shift versions of HMBC spectra have been described using homonuclear broadband decoupling through *J*-resolved spectroscopy [38], pseudo 2D slice-selective (Zangger–Sterk) decoupling [39] or very recently by PSYCHE-decoupling [40]. These spectra are all essentially pseudo 3D experiments, since an additional decoupling dimension is required. Pure shift experiments typically suffer from severe sensitivity losses, which limit their application for carbon-correlated experiments at natural abundance. Real-time BIRD-decoupling [41], which offers the unique feature to enhance both the resolution and sensitivity is possible only for HSQC [42] but not for HMBC experiments. Sensitivity-enhanced homonuclear decoupled HMBC spectra can be obtained by using band-selective decoupling during acquisition [43–46] for a selective region of the proton spectrum [47]. The resolution for the determination of long-range proton–carbon couplings is of course still limited by the signal line-width. We have recently shown that unresolved homonuclear proton scalar couplings can be visualized by real-time *J*-upscaling [48]. This approach enables the determination of scalar coupling constants with high resolution from the direct proton dimension, even in cases of limited digital resolution. Here we show that real-time heteronuclear *J*-upscaled HMBC type spectra can be used to directly visualize small and even unresolved long-range J_{HC} values. To prevent interference from homonuclear coupling it is combined with band-selective decoupling in the proton dimension. With this approach, up to 6-bond splittings (of less than 0.3 Hz) can be observed almost baseline separated.

2. Method

Upscaling of heteronuclear coupling constants has already been used for the indirect dimension of HMBC spectra [28]. Recently we have shown that real-time *J*-upscaling is also possible during detection by repeatedly interrupting the data acquisition and allowing for scalar coupling but not chemical shift evolution during the interruption delay [48]. Interrupted acquisition allows for the manipulation of the size or extent of scalar coupling during the detection, i.e. in real-time [41,42,48–52]. The pulse-sequence of the real-time band-selectively decoupled *J*-upscaled HSQMBC (*J*(up)-HSQMBC) is shown in Fig. 1. Until the start of the acquisition it is a selective HSQMBC (sel-HSQMBC) [53–55], which starts with selective excitation. The pure in-phase character of multiplets is required for homonuclear decoupling, which is used during detection, like in the HOBS-HSQMBC experiment [47]. To understand the evolution behavior of chemical shift as well as homo- and heteronuclear scalar coupling, we can track them individually though the acquisition scheme as shown in Fig. 1c. Homonuclear scalar coupling evolution is refocused in the middle of the inter-

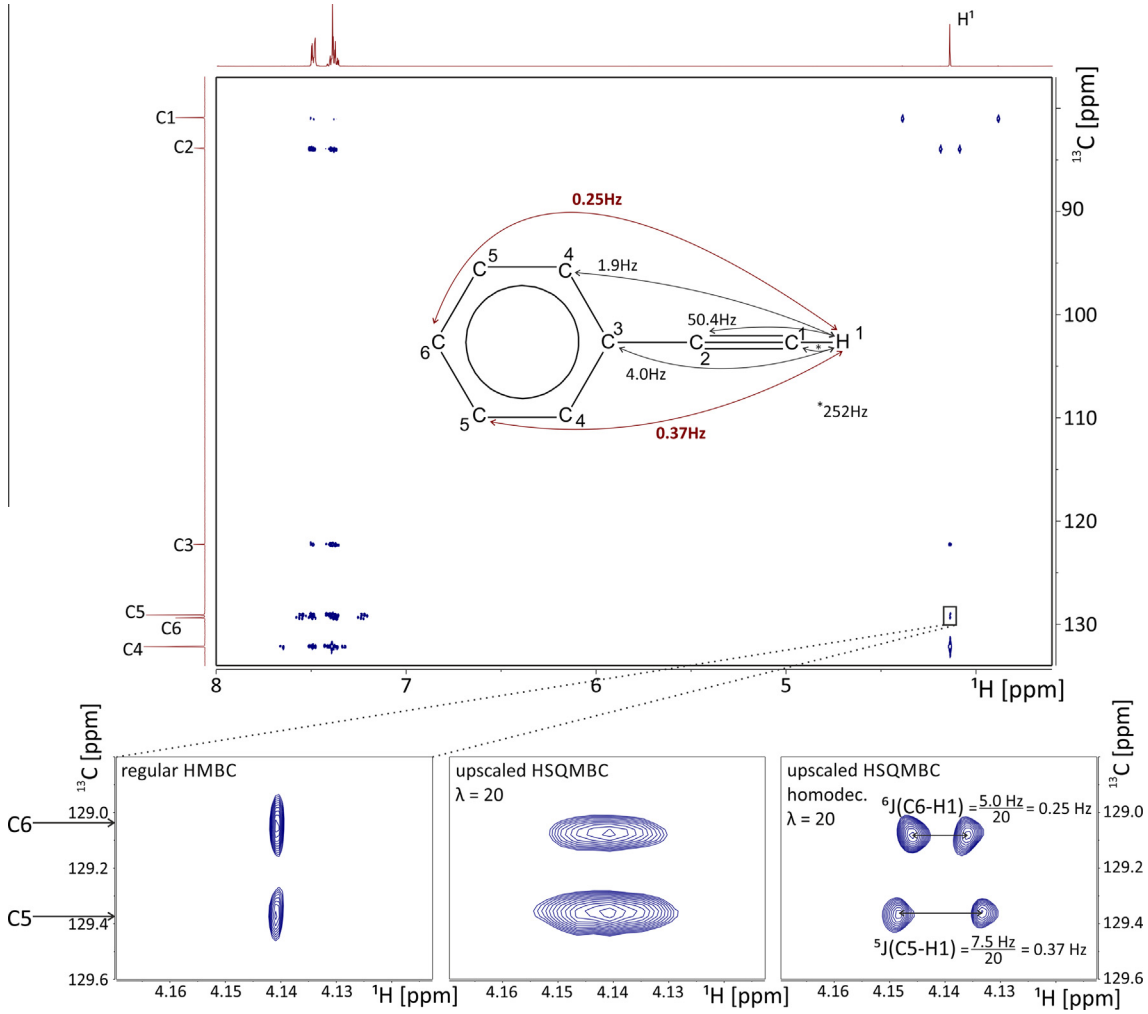

Fig. 2. A conventional HMBC spectrum of phenylacetylene in DMSO-d_6 is shown above. Coupling constants indicated in black in the structure can be obtained from this HMBC. The remaining correlations to C5 and C6 are shown in close-up view below for the conventional magnitude-mode HMBC, a 20-fold J-upscaled HSQMBC and a heteronuclear upscaled and homonuclear band-selectively decoupled HSQMBC. The J-values which could only be determined using this latter spectrum are drawn in red in the structure. The conventional HMBC was recorded with a 16 k $*$ 256 data matrix, 2 scans per increment and a spectral range of 6000–2500 Hz. Zero filling to 32 k and 1 k respectively were performed, after a 60° sine square window function was applied. The upscaled HSQMBC spectra were recorded with 8192 $*$ 256 data points and 16 scans per increment. The spectral range was 6 kHz $*$ 2.5 kHz. Zero filling to 32 k and 2 k data points was performed. (For interpretation of the references to color in this figure legend, the reader is referred to the web version of this article.)

ruption delay by the band-selective proton pulse, whereas heteronuclear coupling continues to evolve by the simultaneous application of a 180° carbon pulse. Chemical shift evolution during the interruption delay is refocused by the central 180° proton pulse. The additional 180° pulse at the beginning of the interruption delay is needed in order to enable continuous chemical shift evolution from one FID chunk to the next. Overall, homonuclear scalar coupling is zero (pure shift), proton chemical shift evolution is unchanged and heteronuclear scalar couplings are enhanced by a user-defined factor λ, which depends on the relative duration of the FID chunk and the interruption delay, according to $J_{\mathrm{eff}} = J \cdot \lambda$, with $\lambda = (2\tau \cdot n/t_2) + 1$. The evolution of chemical shift, homonuclear and heteronuclear scalar coupling during the real-time heteronuclear J-upscaled detection scheme can be described in product operator formalism. The transformations of the individual terms until the middle of the second data chunk is:

$$\hat{I}_x \rightarrow \hat{I}_x * \cos\left(\omega \frac{t_2}{n}\right) - \hat{I}_y * \sin\left(\omega \frac{t_2}{n}\right) \quad \text{Chemical shift evolution}$$

$$\hat{I}_{1x} \rightarrow \hat{I}_{1x} \quad \text{Homonuclear coupling}$$

$$\hat{I}_x \rightarrow \hat{I}_x * \cos\left(\pi J\left(\frac{t_2}{n} + 2\tau\right)\right) - 2\hat{I}_y\hat{S}_z * \sin\left(\pi J\left(\frac{t_2}{n} + 2\tau\right)\right) \quad \text{Heteronuclear coupling}$$

The enhanced resolution of scalar coupling constants by real-time J-upscaling results from the refocusing of magnetic field inhomogeneity effects during the interruption delay. While for large scalar coupling constants line-broadening by residual field inhomogeneity is negligible, it can significantly affect the determination of small coupling constants, even in well-shimmed systems [48]. An additional advantage of real-time J-upscaling is the lower digital resolution needed in the detected dimension since the effective splittings are larger. Chunking artifacts arise in the spectrum around the signals because of residual evolution of homonuclear scalar coupling during the data chunks and the resulting steps between the individual acquisition blocks. The position of these artifacts is at the reciprocal of the data chunking length. By varying the length of the data chunks from scan to scan, the artifacts are reduced significantly [56]. The maximum scaling factor is determined by the relaxation during the interruption. For small mole-

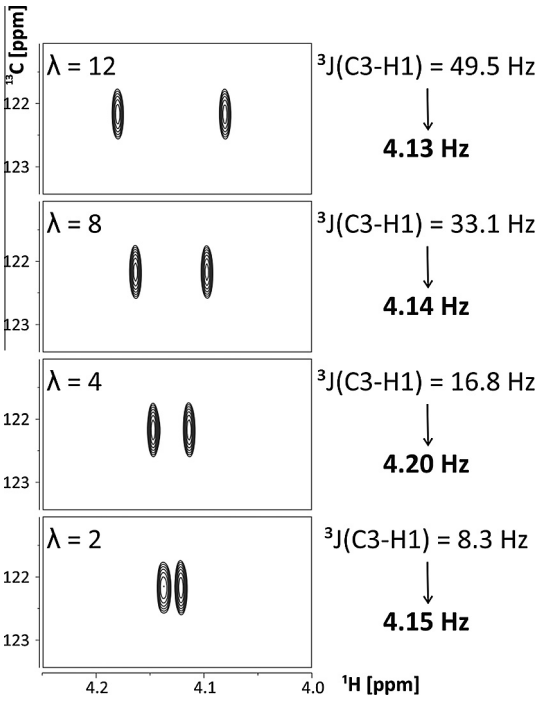

Fig. 3. The C3 region of the H1 phenylacetylene proton with different scaling factors. The cross peak was observed in four *J*(up)-scaled HSQMBC spectra with scaling factors ranging from 2 to 12. The spectra were acquired with a 4 k ∗ 64 data point matrix and variable chunking times between 8 and 10 ms. Zero filling to 16 k and 512 data points was used after the application of a 60° shifted squared sine window function. A spectral range of 9500–2500 Hz and 16 scans per increment were used for all experiments.

cules up to ~20–30-fold is possible. When using larger scaling factors it is necessary to reduce the length of the interruption delay (and in parallel the chunking size), in order to prevent scalar coupling evolution beyond $1/2J$ during 2τ.

3. Results and discussion

To demonstrate the limits of conventional, magnitude mode HMBC experiments [13] and the enhanced scalar coupling resolution of the heteronuclear *J*-upscaled HSQMBC technique, we applied the different experiments on a degassed phenylacetylene sample (50 mg in 600 µl DMSP-d_6). The conventional HMBC is shown in Fig. 2. Correlations for the methine proton at 4.14 ppm are seen to all carbons in phenylacetylene. The one, two and three-bond couplings from H1 to C1 (J = 252 Hz), C2 (J = 50.4 Hz) and C3 (J = 4.0 Hz) can be extracted from a conventional HMBC since H1 does not show any homonuclear couplings in this spectrum. The splitting to C4 (J = 1.9 Hz) can only be seen in a band-selectively decoupled HOBS-HSQMBC after removal of unresolved homonuclear couplings. But also, this very powerful technique fails when dealing with very small heteronuclear coupling constants such as the ones to C5 and C6, due to linewidth limitations. Simple upscaling (with λ = 20) of a HSQMBC yields very broad peaks due to the combination of small homo- and heteronuclear couplings. However, the combination of band-selective decoupling with *J* upscaling provides the resolution necessary to determine the remaining five- and six-bond couplings to C5 (J = 0.37 Hz) and C6 (J = 0.25 Hz). Twenty-fold real-time upscaling allowed these couplings to be visualized in the direct dimension baseline-separated, while they are hidden in the linewidth of a conventional HMBC and even a homonuclear decoupled HSQMBC.

Upscaling does increase the linewidth as can be seen in Fig. 2, but not by as much as the coupling is upscaled. Due to this broadening the intensities are also reduced compared to a conventional HMBC. However, band-selective decoupling increases the intensity by collapsing homonuclear splittings, like in the HOBS-HSQMBC. To demonstrate the validity of the coupling constants obtained from the upscaled HMBC spectra, a signal whose coupling constant could be extracted from a conventional HMBC has been upscaled. The C3–H1 cross peak of phenylacetylene shows a splitting of 4.0 Hz in a conventional NMR experiment. In Fig. 3 upscaled spectra of this cross peak are shown with λ ranging from 2 to 12. By dividing the measured coupling constant by the corresponding scaling factor the results are only varying by 0.07 Hz, with an average of 4.15. The slightly larger value compared to the 4.0 Hz obtained from a magnitude-mode conventional HMBC probably results from the broad components of the doublet in the latter spectrum, which leads to extracted coupling constants which are smaller than their actual values.

One limiting factor of real-time *J*-upscaling experiments is the data chunk duration. We used a chunking length of approximately 10 ms, which allows upscaled coupling constants of up to 100 Hz (=1/10 ms) to be measured. A larger splitting would show the same

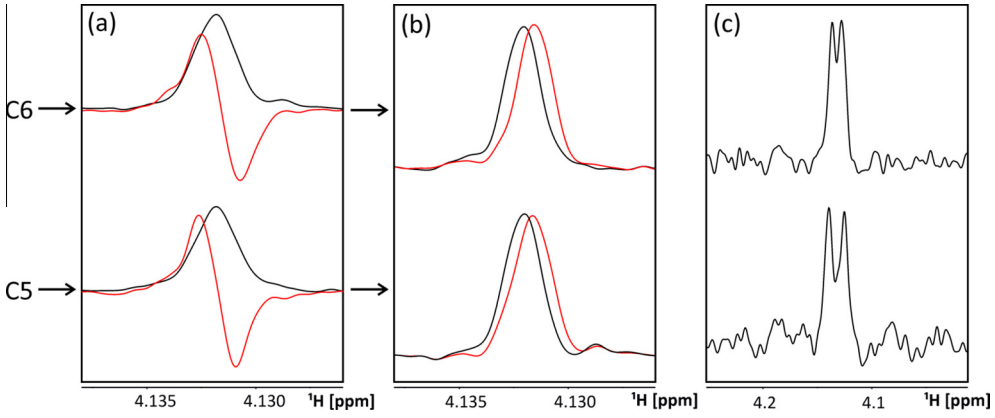

Fig. 4. (a) F2-traces of C6 and C5 of an in-phase (black) and anti-phase (red) HOBS-HSQMBC. The HOBS-HSQMBC was recorded with 32 k data points and a data chunking length of 35 ms. 64 increments were used in the indirect dimension. Zero filling to 256 k and 512 data points was performed after multiplication with a 60° shifted squared sine bell window function. (b) The peak shift of the addition (black) and subtraction (red) of both traces corresponds to the coupling constant of the peak (^6J = 0.21 Hz, ^5J = 0.18 Hz). (c) in comparison the corresponding traces from a *J*(up)-scaled HSQMBC (^6J = 0.21 Hz, ^5J = 0.35 Hz). These spectra had a 4 k ∗ 64 data point matrix and a variable chunking time between 30 and 35 ms. Zero filling to 32 k ∗ 256 data points was performed after a 60° shifted squared sine bell window function was applied. A shaped 180° 5 ms Gauss pulse was used for band selective excitation and a spectral range of 6000–700 Hz was used for all experiments. 16 scans were recorded for each increment of all spectra. (For interpretation of the references to color in this figure legend, the reader is referred to the web version of this article.)

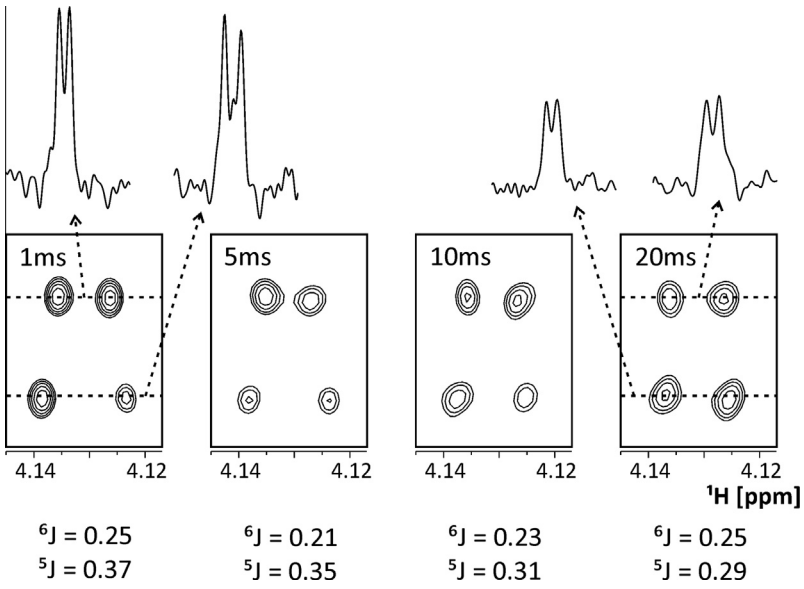

Fig. 5. C6 and C5 correlations to H1 of phenylacetylene acquired with different Gauss pulse lengths. The measured coupling constants (in Hertz) of the different pulse duration experiments are shown below the spectra. F2-traces of the 1 ms and 20 ms Gauss experiments are plotted above the 2D spectra to show the reduction in intensity upon the use of longer, more selective, pulses. All spectra were recorded with 4 k * 64 data points and data chunking times between 30 and 35 ms.

evolution as a correspondingly smaller splitting according to the Nyquist theorem. Therefore, the maximum scaling factor that can be used depends on the size of the actual coupling. Signals with smaller *J*-values can be upscaled with larger λ values. Additionally, artifacts are becoming more severe with increasing scaling factor. To get an idea of the sensitivity penalty and artifact evolution during *J*(up)-scaling the C4–H1 correlation is compared in Supporting Fig. S1 without and with 20-fold upscaling. Although the signal intensity has dropped by a factor of 4 the extracted coupling constant is the same. In general, the amount of signal reduction depends not only on the scaling factor, but also the transverse relaxation time of the investigated signal. For slowly relaxing signals the reduction is lower [48]. Small heteronuclear coupling constants can also be determined by in-phase–anti-phase (IPAP) type spectra, as implemented in the HOBS-HSQMBC sequence [47]. To compare the potential of the *J*(up)-HSQMBC versus an IPAP HOBS-HSQMBC we applied the latter technique to the H1–C5 and H1–C6 couplings of phenylacetylene. The F2-traces of the in-phase spectrum (black) and an anti-phase spectrum (red) are shown in Fig. 4a. The heteronuclear scaling coupling constant is obtained by measuring the shift difference between the addition (black) and subtraction (red) of the two individual traces (Fig. 4b).

The signal splittings obtained for very small coupling constants from an IPAP-HOBS-HSQMBC depends heavily on the data processing, in particular the phasing. Small differences in the phasing yield huge differences in the extracted signal splitting. Additionally, the weighting of both traces is quite tricky, as differences in the relative weighting of the in-phase and anti-phase signal also have a huge impact on the relative size of such small *J* values. The IPAP HOBS-HSQMBC yielded coupling constants of $^{6}J = 0.21$ Hz and $^{5}J = 0.18$ Hz, which are not only quite different from the ones obtained using *J*(up)-HSQMBC, but also (unrealistically) larger for the 6-bond compared to the 5-bond couplings. It should also be mentioned that the quantitative HMBC approach proved completely unreliable in an attempt to measure these small 5- and 6-bond couplings because after the very long coupling evolution delay needed there was basically no signal left due to relaxation losses. For well isolated proton signals, relatively short selective pulses can be used for decoupling during acquisition to keep relaxation losses during the interruptions to a minimum. The use of longer, more selective, pulses leads to broader signals due to faster relaxation during acquisition. However, Gaussian pulses of up to 20 ms (corresponding to an excitation width of 45 Hz) allow the extraction of *J* values below 0.3 Hz in a 20-fold upscaled spectrum (Fig. 5). The signal intensities decrease upon increasing pulse selectivity.

For singlet proton signals without any other proton coupling partners, homonuclear decoupling is of course not necessary. An example is the application of the *J*(up)-HSQMBC for the measurement of two- and three-bond proton-carbon couplings of the central proton of the dye D131 (2-Cyano-3-[4-[4-(2,2-diphenylethenyl)phenyl]-1,2,3,3a,4,8b-hexahydrocyclopent[b]indol-7-yl]-2-propenoic acid) [15 mg in 600 µl pyridine-d_5] in Fig. 6. For the assignment of the (2,2-diphenylethenyl)phenyl moiety, especially the stereospecific assignment of the phenyl rings b and c, the correlations of the locally isolated central hydrogen at 7.21 ppm to the phenyl and ethenyl carbons was key. In a conventional HMBC the correlations to C1b and C1c both show a splitting (9.2 and 7.2 Hz). However, the direct measurement of coupling constants would not be very accurate due to the rather broad doublet signals. The coupling to C2 is not resolved in an HMBC, and in the HOBS-HSQMBC the value is too small (1.9 Hz) because the splitting value is close to the linewidth. By upscaling the HSQMBC spectrum to $\lambda = 4$ not only the doublet to C1c is properly defined ($^{3}J = 7.0$ Hz), it is now also possible to measure the coupling constant to C2 ($^{2}J = 2.6$ Hz). All two- and three-bond coupling constants, which were essential for the full assignment, especially of the individual aromatic rings are indicated in Fig. 6. It might be worth mentioning, that in this case homonuclear band-selective decoupling does not improve the quality of the spectrum, because the long-range coupled protons are too close in frequency and the necessary selective pulse would be too long.

4. Conclusion

In conclusion we have presented a method to record "real-time" heteronuclear *J*-upscaled HSQMBC spectra. This technique minimizes the effect of magnetic field inhomogeneities on scalar coupling and allows their direct visualization in cases where the splitting is hidden in the signal linewidth or is unresolved due to a limited digital resolution of a spectrum.

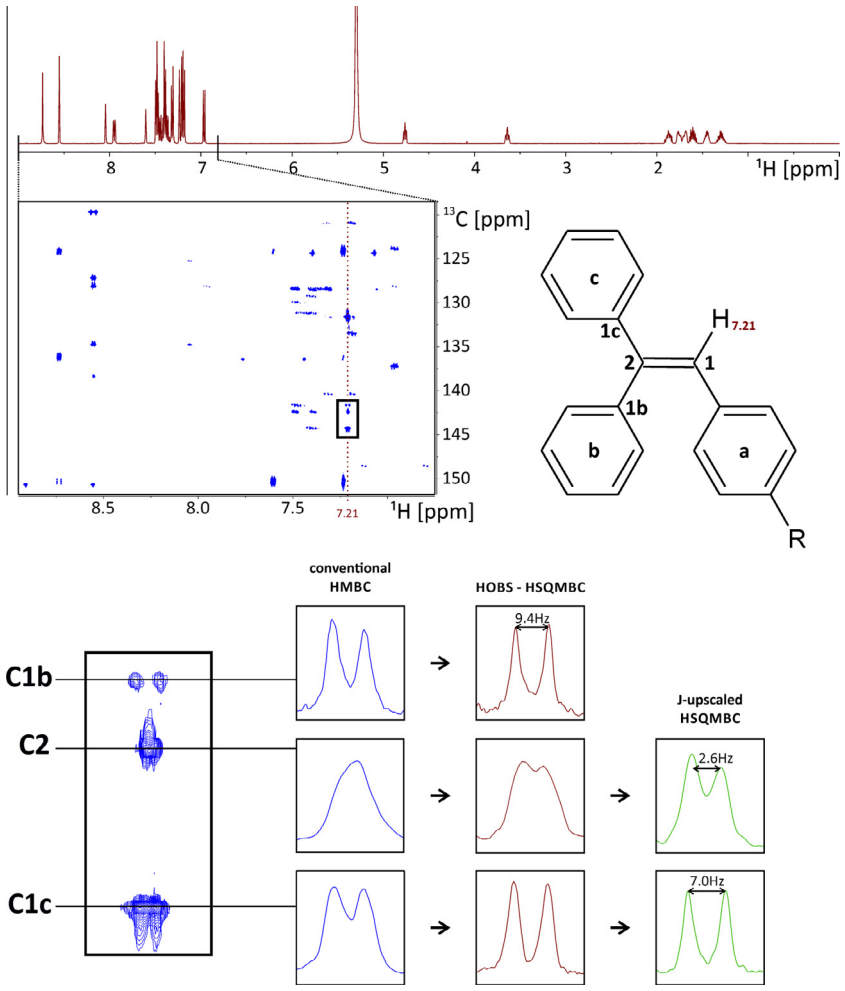

Fig. 6. A zoom of the terminal aromatic region of an HMBC of the dye D131 (15 mg in pyridine-d_5) is shown above, together with the structure of the aromatic moiety. Selected traces of a regular HMBC spectrum (in blue) can be compared with a HOBS-HSQMBC [47] in red and a fourfold J(up)-HSQMBC in green. Only in the J(up)-HSQMBC it is possible to measure the relatively small two bond heteronuclear coupling constant of 2.6 Hz. The observed region of the upscaled traces are also expanded by the factor λ, for a direct comparison of the resolution enhancement. For the conventional HMBC a 16 k $*$ 256 data matrix and a spectral range of 6000–5000 was used with 16 scans per increment. Zero filling to 32 k $*$ 523 data points was performed. For the HOBS-HSQMBC 16 k $*$ 128 data points for a spectral range of 5500–7500 Hz were recorded and zero filled to 32 k $*$ 512. The J(up)-scaled HSQMBC was recorded with 2 k $*$ 96 data points and a spectral range of 5500–4400 Hz. Zero filling to 32 k $*$ 512 was performed. (For interpretation of the references to color in this figure legend, the reader is referred to the web version of this article.)

5. Experimental

All experiments were carried out on a Bruker Avance III 500 MHz spectrometer using a 5 mm TXI probe with z-axis gradients at 298 K. All chemicals were purchased from Sigma Aldrich at 98% purity or above. For the band selective excitation/refocusing of the protons a 1 ms 180° Gauss pulse was used. Sine shapes were used for all pulsed field gradients. Further experimental details are given for the respective spectra.

Appendix A. Supplementary material

Supplementary data associated with this article can be found, in the online version, at http://dx.doi.org/10.1016/j.jmr.2016.05.002.

References

[1] M. Karplus, Vicinal proton coupling in nuclear magnetic resonance, J. Am. Chem. Soc. 85 (18) (1963) 2870–2871.
[2] T. Parella, J.F. Espinosa, Long-range proton-carbon coupling constants: NMR methods and applications, Prog. NMR Spectrosc. 73 (2013) 17–55.
[3] J.L. Marshall, Carbon-Carbon and Carbon-Proton NMR Couplings: Applications to Organic Stereochemistry and Conformational Analysis, Ed. Verlag Chemie Int., 1983.
[4] P.E. Hansen, Carbon—hydrogen spin—spin coupling constants, Prog. NMR Spectrosc. 14 (4) (1981) 175–295.
[5] T. Parella, Pulsed field gradients: a new tool for routine NMR, Magn. Reson. Chem. 36 (1998) 467–557.
[6] W.A. Thomas, Unravelling molecular structure and conformation—the modern role of coupling constants, Prog. NMR Spectrosc. 30 (3–4) (1997) 183–207.
[7] B.L. Marquez, W.H. Gerwick, R. Thomas Williamson, Survey of NMR experiments for the determination of ^{n}J(C, H) heteronuclear coupling constants in small molecules, Magn. Reson. Chem. 39 (9) (2001) 499–530.
[8] G.T. Montelione, M.E. Winkler, P. Rauenbuehler, G. Wagner, Accurate measurements of long-range heteronuclear coupling constants from homonuclear 2D NMR spectra of isotope-enriched proteins, J. Magn. Reson. 82 (1) (1989) 198–204.
[9] D. Uhrın, G. Batta, V.J. Hruby, P.N. Barlow, K.E. Kövér, Sensitivity- and gradient-enhanced hetero (ω1) half-filtered TOCSY experiment for measuring long-range heteronuclear coupling constants, J. Magn. Reson. 130 (2) (1998) 155–161.
[10] M. Kurz, P. Schmieder, H. Kessler, HETLOC, an efficient method for determining heteronuclear long-range couplings with heteronuclei in natural abundance, Angew. Chem. Int. Ed. Engl. 30 (10) (1991) 1329–1331.
[11] A. Bax, S. Subramanian, Sensitivity-enhanced two-dimensional heteronuclear shift correlation NMR spectroscopy, J. Magn. Reson. 67 (3) (1986) 565–569.
[12] G. Otting, H. Senn, G. Wagner, K. Wüthrich, Editing of 2D ^{1}H NMR spectra using X half-filters. Combined use with residue-selective ^{15}N labeling of proteins, J. Magn. Reson. 70 (3) (1986) 500–505.

[13] A. Bax, M.F. Summers, Proton and carbon-13 assignments from sensitivity-enhanced detection of heteronuclear multiple-bond connectivity by 2D multiple quantum NMR, J. Am. Chem. Soc. 108 (8) (1986) 2093–2094.
[14] J.J. Titman, D. Neuhaus, J. Keeler, Measurement of long-range heteronuclear coupling constants, J. Magn. Reson. 85 (1) (1989) 111–131.
[15] J.M. Richardson, J.J. Titman, J. Keeler, D. Neuhaus, Assessment of a method for the measurement of long-range heteronuclear coupling constants, J. Magn. Reson. 93 (3) (1991) 533–553.
[16] S. Sheng, H. van Halbeek, Accurate and precise measurement of heteronuclear long-range couplings by a gradient-enhanced two-dimensional multiple-bond correlation experiment, J. Magn. Reson. 130 (2) (1998) 296–299.
[17] J. Keeler, D. Neuhaus, J.J. Titman, A convenient technique for the measurement and assignment of long-range carbon-13 proton coupling constants, Chem. Phys. Lett. 146 (6) (1988) 545–548.
[18] D. Bruhwiler, G. Wagner, Selective excitation of H-1 resonances coupled to C-13-hetero COSY and relay experiments with H-1 detection for a protein, J. Magn. Reson. 69 (1986) 546–551.
[19] B.K. John, D. Plant, R.E. Hurd, Improved proton-detected heteronuclear correlation using gradient-enhanced z and zz filters, J. Magn. Reson. Ser. A 101 (1) (1993) 113–117.
[20] S. Boros, K.E. Kövér, Low-power composite CPMG HSQMBC experiment for accurate measurement of long-range heteronuclear coupling constants, Magn. Reson. Chem. 49 (3) (2011) 106–110.
[21] H. Koskela, I. Kilpeläinen, S. Heikkinen, LR-CAHSQC: an application of a Carr–Purcell–Meiboom–Gill-type sequence to heteronuclear multiple bond correlation spectroscopy, J. Magn. Reson. 164 (2) (2003) 228–232.
[22] K.E. Kövér, G. Batta, K. Fehér, Accurate measurement of long-range heteronuclear coupling constants from undistorted multiplets of an enhanced CPMG-HSQMBC experiment, J. Magn. Reson. 181 (1) (2006) 89–97.
[23] K.E. Kövér, O. Prakash, V.J. Hruby, Improved 2D inverse proton detected C, H correlation NMR techniques for the total assignment of carbon resonances of a highly delta opioid receptor agonist peptide, Magn. Reson. Chem. 31 (3) (1993) 231–237.
[24] V. Lacerda, Gil V.J. da Silva, M.G. Constantino, C.F. Tormena, R.T. Williamson, B. L. Marquez, Long-range *J*(CH) heteronuclear coupling constants in cyclopentane derivatives, Magn. Reson. Chem. 44 (1) (2006) 95–98.
[25] R. Marek, L. Králík, V. Sklenář, Gradient-enhanced HSQC experiments for phase-sensitive detection of multiple bond interactions, Tetrahedron Lett. 38 (4) (1997) 665–668.
[26] R.T. Williamson, B.L. Marquez, W.H. Gerwick, K.E. Kövér, One- and two-dimensional gradient-selected HSQMBC NMR experiments for the efficient analysis of long-range heteronuclear coupling constants, Magn. Reson. Chem. 38 (2000) 264–273.
[27] S. Gil, J.F. Espinosa, T. Parella, IPAP-HSQMBC: measurement of long-range heteronuclear coupling constants from spin-state selective multiplets, J. Magn. Reson. 207 (2) (2010) 312–321.
[28] K. Furihata, H. Seto, J-Resolved HMBC, a new NMR technique for measuring heteronuclear long-range coupling constants, Tetrahedron Lett. 40 (34) (1999) 6271–6275.
[29] C.E. Hadden, G.E. Martin, V.V. Krishnamurthy, Improved performance accordion heteronuclear multiple-bond correlation spectroscopy-IMPEACH-MBC, J. Magn. Reson. 140 (1) (1999) 274–280.
[30] G.E. Martin, C.E. Hadden, R.C. Crouch, V.V. Krishnamurthy, ACCORD-HMBC: advantages and disadvantages of static versus accordion excitation, Magn. Reson. Chem. 37 (1999) 517–528.
[31] G.A. Zhu, A. Renwick, A. Bax, Measurement of two- and three-bond ^{1}H-^{13}C *J*-couplings from quantitative heteronuclear *J* correlation for molecules with overlapping ^{1}H resonances, using t_1 noise reduction, J. Magn. Reson. Ser. A 110 (2) (1994) 257–261.
[32] G. Zhu, A. Bax, Measurement of long-range ^{1}H–^{13}C coupling constants from quantitative 2D heteronuclear multiple-quantum correlation spectra, J. Magn. Reson. Ser. A 104 (3) (1993) 353–357.
[33] J.A. Aguilar, S. Faulkner, M. Nilsson, G.A. Morris, Pure shift ^{1}H NMR: a resolution of the resolution problem?, Angew Chem. Int. Ed. Engl. 49 (23) (2010) 3901–3903.
[34] R.W. Adams, Pure shift NMR spectroscopy, in: R.K. Harris, R.L. Wasylishen (Eds.), eMagRes, John Wiley & Sons Ltd., Chichester, UK, 2007, pp. 295–310.
[35] L. Castañar, T. Parella, Broadband ^{1}H homodecoupled NMR experiments: recent developments, methods and applications, Magn. Reson. Chem. 53 (6) (2015) 399–426.
[36] N.H. Meyer, K. Zangger, Boosting the resolution of ^{1}H NMR spectra by homonuclear broadband decoupling, ChemPhysChem 15 (1) (2014) 49–55.
[37] K. Zangger, Pure shift NMR, Prog. NMR Spectrosc. 86–87 (2015) 1–20.
[38] P. Sakhaii, B. Haase, W. Bermel, Broadband homodecoupled heteronuclear multiple bond correlation spectroscopy, J. Magn. Reson. 228 (2013) 125–129.
[39] I. Timári, T.Z. Illyés, R.W. Adams, M. Nilsson, L. Szilágyi, G.A. Morris, K.E. Kövér, Precise measurement of long-range heteronuclear coupling constants by a novel broadband proton-proton-decoupled CPMG-HSQMBC method, Chem.-Eur. J. 21 (8) (2015) 3472–3479.
[40] I. Timári, L. Szilágyi, K.E. Kövér, PSYCHE CPMG-HSQMBC: an NMR spectroscopic method for precise and simple measurement of long-range heteronuclear coupling constants, Chem.-Eur. J. 21 (40) (2015) 13939–13942.
[41] A. Lupulescu, G.L. Olsen, L. Frydman, Toward single-shot pure-shift solution ^{1}H NMR by trains of BIRD-based homonuclear decoupling, J. Magn. Reson. 218 (2012) 141–146.
[42] L. Paudel, R.W. Adams, P. Király, J.A. Aguilar, M. Foroozandeh, M.J. Cliff, M. Nilsson, P. Sándor, J.P. Waltho, G.A. Morris, Simultaneously enhancing spectral resolution and sensitivity in heteronuclear correlation NMR spectroscopy, Angew. Chem. Int. Ed. Engl. 52 (44) (2013) 11616–11619.
[43] Veera Mohana Rao Kakita, J. Bharatam, Real-time homonuclear broadband and band-selective decoupled pure-shift ROESY, Magn. Reson. Chem. 52 (7) (2014) 389–394.
[44] J.M. McKenna, J.A. Parkinson, HOBS methods for enhancing resolution and sensitivity in small DNA oligonucleotide NMR studies, Magn. Reson. Chem. 53 (4) (2015) 249–255.
[45] J. Ying, J. Roche, A. Bax, Homonuclear decoupling for enhancing resolution and sensitivity in NOE and RDC measurements of peptides and proteins, J. Magn. Reson. 241 (2014) 97–102.
[46] L. Castañar, P. Nolis, A. Virgili, T. Parella, Full sensitivity and enhanced resolution in homodecoupled band-selective NMR experiments, Chem.-Eur. J. 19 (51) (2013) 17283–17286.
[47] L. Castañar, J. Saurí, P. Nolis, A. Virgili, T. Parella, Implementing homo- and heterodecoupling in region-selective HSQMBC experiments, J. Magn. Reson. 238 (2014) 63–69.
[48] S. Glanzer, K. Zangger, Visualizing unresolved scalar couplings by real-time J-upscaled NMR, J. Am. Chem. Soc. 137 (15) (2015) 5163–5169.
[49] N.H. Meyer, K. Zangger, Simplifying proton NMR spectra by instant homonuclear broadband decoupling, Angew. Chem. Int. Ed. Engl. 52 (28) (2013) 7143–7146.
[50] N. Gubensäk, Walter M.F. Fabian, K. Zangger, Disentangling scalar coupling patterns by real-time SERF NMR, Chem. Commun. 50 (82) (2014) 12254–12257.
[51] N. Lokesh, S.R. Chaudhari, N. Suryaprakash, Quick re-introduction of selective scalar interactions in a pure-shift NMR spectrum, Chem. Commun. 50 (98) (2014) 15597–15600.
[52] S. Glanzer, K. Zangger, Uniform reduction of scalar coupling by real-time homonuclear J-downscaled NMR, ChemPhysChem 16 (15) (2015) 3313–3317.
[53] S. Gil, J.F. Espinosa, T. Parella, Accurate measurement of small heteronuclear coupling constants from pure-phase α/β HSQMBC cross-peaks, J. Magn. Reson. 213 (1) (2011) 145–150.
[54] J.F. Espinosa, P. Vidal, T. Parella, S. Gil, Measurement of long-range proton-carbon coupling constants from pure in-phase 1D multiplets, Magn. Reson. Chem. 49 (8) (2011) 502–507.
[55] J. Saurí, T. Parella, J.F. Espinosa, CLIP-HSQMBC: easy measurement of small proton-carbon coupling constants in organic molecules, Org. Biomol. Chem. 11 (27) (2013) 4473–4478.
[56] J. Mauhart, S. Glanzer, P. Sakhaii, W. Bermel, K. Zangger, Faster and cleaner real-time pure shift NMR experiments, J. Magn. Reson. 259 (2015) 207–215.